Hindawi
Shock and Vibration
Volume 2020, Article ID 5952796, 11 pages
https://doi.org/10.1155/2020/5952796

Research Article

Radial Joints Behavior of a Precast Asymmetric Underpass Induced by Long-Term Loads of Ground Vehicles

Zhiyi Jin, Taiyue Qi, Xiao Liang, Bo Lei, Yangyang Yu, Yuchen Gong, and Weidu Ji

Key Laboratory of Transportation Tunnel Engineering, Ministry of Education, Southwest Jiaotong University, Chengdu 610031, China

Correspondence should be addressed to Taiyue Qi; qitaiyue58@126.com

Received 10 July 2019; Revised 13 January 2020; Accepted 10 February 2020; Published 23 March 2020

Academic Editor: Marco Lepidi

With the rapid development of the urbanization, many underpasses are designed and constructed in big cities to alleviate the huge traffic pressure. The construction method has been changed from traditional on-site concrete pouring technology to prefabricated assembly technology. However, this change will inevitably bring out some new problems to be studied such as the behaviour of the radial joints. In this study, the numerical simulation model of Moziqiao precast and assemble underpass with large asymmetric cross section was constructed by using the ABAQUS software to study the transient response of the underpass induced by ground surface dynamic load. Based on the similarity theory a 1/10 scaled model test was carried out to study the long-term radial joint behaviour of the underpass considering the prestress loss during the 2000 000 loading cycles. The results transient dynamic response from computed and tested was compared in terms of acceleration. The comparison showed that the transient response accelerations have good consistency. The results of the physical model test were analysed in terms of joint opening, closure, and slipping. The accumulative joint opening was closely correlated to the prestress level, and the joint opening at different prestress levels increased with the loss of the prestress. The joints closure decreased with the increase of the previous accumulative color value. The joint slipping mainly attributed to the slipping of the top segment. Both the opening and slipping of the joints at RJ 1 were larger than that of RJ3 due to the wider span of RJ1, which reflected an asymmetric effect. This study revealed the long-term accumulative behaviour of the radial joints, which convinced us that the long-term accumulative deformation of the joints should be taken into consideration during the design stage for similar projects.

1. Introduction

The rapid growth of population in big cities has led to the urban ground traffic more and more crowded [1–3]. Hence, different kinds of underground structures and spaces such as metro tunnels, metro stations, utility tunnels, underground shelters, and underpasses may appear in any large city. Underpasses constructed crossing underneath highways in downtown areas will become common. The underpass structure will lose its function partly or completely due to long-term repeated vibration from the ground surface vehicles. The vehicle dynamic loads can affect the underpasses within the depth of 14 m, and the effect decreases with the increase of distance from the excitation source [4]. Therefore, the long-term dynamic effect on underpasses induced by ground surface vehicles cannot be neglected during the design stage.

Typically, cut-and-cover underpasses are often box shaped and constructed by using cast-in-place reinforced concrete liners. Compared with cast-in-place concrete, precast structure has higher prefabrication precision and faster construction speed [5–9]. The prefabrication technology was used in Sendai subway in Japan and Tashkent subway in Uzbekistan decades ago [10–12]. For those advantages of precast concrete, the next decade is likely to witness a considerable rise of precast underpass in urban areas. Although the prefabrication concrete is a promising alternative to the traditional cast-in-place concrete, the main problem in its use in underpass is the size and weight cannot exceed the transport and crane ability under

current conditions. Therefore, the large cross-section underpass must be divided into segments [13]. Radial joints (RJs) are used to connect adjacent segments in the underpass lining [14]. Radial joints have two main functions for precast tunnel linings, one is transferring loads and the other is a sealant of the structure. The radial joint is the potential weakest link of the tunnel compared to the segment itself due to the lower stiffness [15–17]. Radial joints are not only the weak position of structural deformation but also the high incidence of tunnel distress [18, 19].

It has been presented in different papers that the radial joints have a prominent influence on the tunnel deformation. Wang et al. [20] found that the variation of tunnel diameter is closely related to the opening of radial joints by using a simplified method to evaluate the deformation of a shield tunnel in soft soil in Shanghai. From a field case study of an operated metro tunnel under surface surcharge load, Huang et al. [21] found that the convergence of the tunnel is closely correlate to the radial joint width and less correlate to the deformation of the circumferential joint. Yi et al. [22] carried out a model experiment to study the accumulative deformation of a metro tunnel lining induced by dynamic load from the abovementioned high-speed train and indicated that the main contribution of the accumulative deformation of the tunnel lining came from the opening and dislocation of the joints. All these studies above showed that the behavior of radial joints play an important role in tunnel deformation.

For this reason, numerous studies focused on radial joints behavior. Jin et al. [23] conducted a series of full-scale experiments to investigate the joint behavior of a water-conveyance tunnel. Caratelli et al. [14] performed a test on two steel fiber reinforced concrete elements to study the behavior of longitudinal joints of a shield tunnel lining and interpreted the behavior in an analytical manner. Liu et al. [24] through a full-scale test (with a whole ring) to investigate the ultimate bearing capacity of a shield tunnel in Shanghai, the test result showed that the lining failure was caused by joints failure. However, these studies mainly focused on the behavior of shield tunnel and the loading conditions on static loads.

Although many research achievements were realized on the joint behavior of shield tunnel linings under different kinds of load conditions in the abovementioned references, the long-term joint behavior of shallow buried underpass linings induced by ground surface vehicle dynamic load is still not clear. Motivated by this research status, this paper tries to make a thorough understanding of the effect of long-term ground surface vehicle loads on the radial joint behavior of prefabricated and assemble underpass. Taking the Moziqiao underpass in Chengdu as an engineering background, a numerical model was constructed to study the transient dynamic response of the structure, and 1/10 scaled model experiment were carried out to study the long-term accumulative deformation of the joints. According to the measured joint deformation data of the model experiment, characters of joint displacement were analyzed.

2. Engineering Background

In the case of Moziqiao underpass crossing beneath the south section of the first ring road in Chengdu, the location of the project can be seen in Figure 1. The project is designed to relieve the heavy traffic in downtown Chengdu. The underpass consists of two tubes, one is 3-passing lane with a width of 11.85 m and the other is 2-passing lane with a width of 8.35 m. The length of the project is 200 m and the height of the underpass is 8.2 m. The thickness of the plain fill is 3 m. The cross section of the underpass is 178.3 m^2 and the cross section must be partitioned into segments. The partition scheme was chosen by considering the internal force distribution, amounts of joints, and construction time. The final partition scheme of the underpass was that the structure was cut at the middle in the height direction, as shown in Figure 2(a). The sketch of the project can be seen in Figure 2(b).

The strength of the prefabricated concrete lining is C50. The mechanical and physical parameters of the plain fill and concrete lining are shown in Tables 1 and 2, respectively.

The dynamic load induced by the vehicle moving on the ground surface is not obvious due to the speed of the vehicles is far slower than the wave velocity of the highway surface. Therefore, the influence of moving vehicle on the dynamic response of the ground surface can be neglected if the pavement is even enough. However, the pavement of any highway cannot be fully level, and the pavement evenness becomes worse with the service time. It can be considered that the vertical vibration of vehicles is completely caused by the unevenness of the ground surface [25–27]. A harmonic load model which can reflect the vehicle moving velocity and pavement unevenness was used to describe the vibration induced by highway vehicle by Chen [28], according to the simplified form of dynamic load, the cyclic load can be expressed in the form of

$$F(t) = P - \cos\left(2 \times \pi \times \frac{v}{l} \times t\right), \tag{1}$$

where P is the amplitude of the dynamic load, assumed equal to 150 kN, (v/l) is the frequency of dynamic load, v is the maximum vehicle velocity of the ground surface, assumed as 12 m/s, and l is the wavelength of the pavement, assumed as 20 m. Hence, equation (1) can be further simplified as

$$F(t) = P - \cos(2 \times \pi \times 0.6 \times t). \tag{2}$$

3. Numerical and Physical Experiment Setups

3.1. Numerical Model Setup. In order to study the behavior of the underpass radial joints under dynamic load, a 3D numerical model with the real project was constructed using finite element software ABAQUS 2016.

The flat radial joints were adopted in numerical modelling, and connecters between the underpass segments were not considered. There are two shear keys which are installed at each radial joint.

The dimension of the model is 10 m in length (in the axial direction of the tunnel), 43.8 m in width, and 21.7 m in

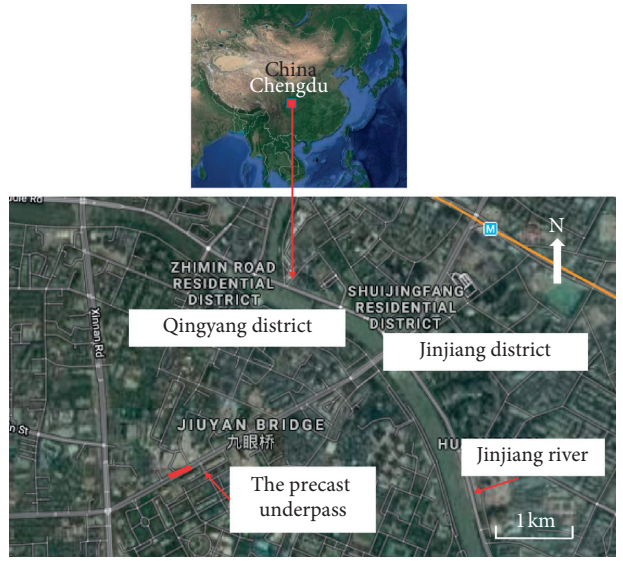

Figure 1: Project location (map data from Google earth).

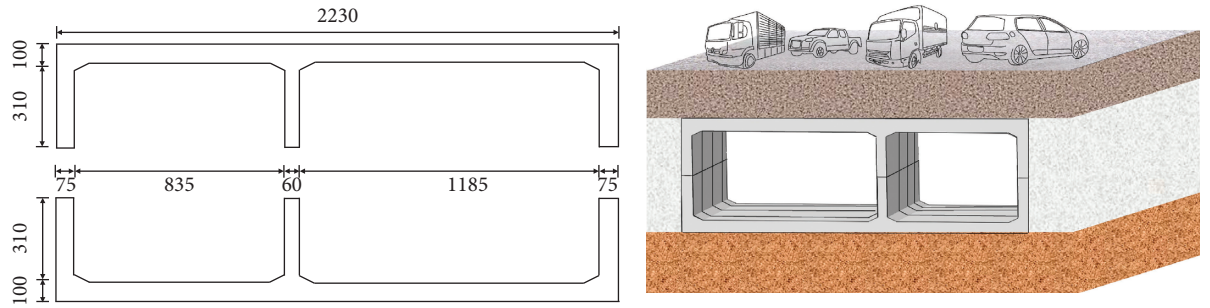

(a) (b)

Figure 2: Partition scheme and sketch of the structure. (a) Partition scheme of the structure. (b) Sketch of the project.

Table 1: The mechanical parameters of segments in the prototype and model.

Parameters Unite	Density (kg/m^3)	Elastic modulus (MPa)	Poison's ratio —	Tensile strength (MPa)	Compressive strength (MPa)
Prototype	2600	34500	0.21	2.64	32.4
Model	2600	3450	0.21	0.264	3.24

Table 2: The mechanical parameters of backfill soil in the prototype and model.

Parameters Unite	Thickness (m)	Density (kg/m^3)	Elastic modulus (MPa)	Poison's ratio —	Friction angle (°)	Cohesion (KPa)
Prototype	3	1910	10.15	0.32	18.1	17.5
Model	0.3	1900	1.01	0.32	18	17

height. The geometry of the model is shown in Figure 3(a). The whole model contains soils, plain concrete, and tunnel. Figure 3(b) plotted the segments and shear keys of the tunnel.

The type "hard contact" [29] model was used to simulate the interaction between contact surfaces of segments. This kind of contact does not allow segment penetrate to each other at the compression state. The friction coefficient was set at 0.4, according to laboratory test. Contact surfaces between shear keys and tunnel segments were set as surface-to-surface contact type and the friction coefficient was set at 0.2. The "tie" mode was used to define the interaction between soil and the underpass lining. Parameters in the numerical model were the same as the real project as listed in Tables 1 and 3. In the finite element model prestress mentioned in Section 2 was applied by 5 pairs of

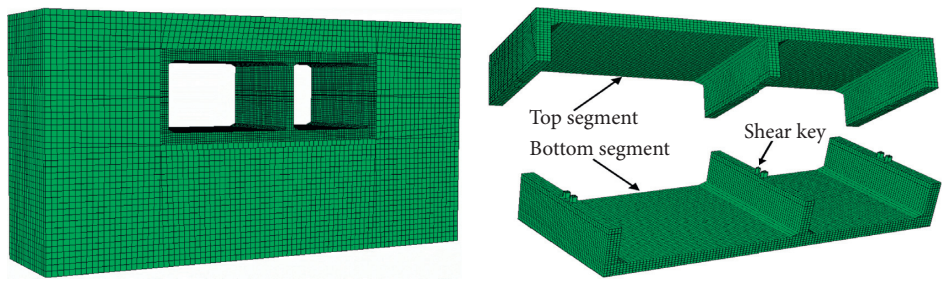

Figure 3: Numerical modelling. (a) The whole model. (b) The segments and shear keys.

Table 3: Similitude ratio of the physical quantities.

Quantities	Similarity relation	Ratio
Length	$C_l = l_p/l_m$	10
Density	$C_\rho = \rho_p/\rho_m$	1
Elastic modulus	$C_E = E_p/E_m$	10
Stress	$C_\sigma = \sigma_p/\sigma_m$	10
Cohesion	$C_c = C_p/C_m$	10
Frequency	$C_f = f_P/f_m$	0.316
Friction angle	$C_\varphi = \varphi_p/\varphi_m$	1
Strain	$C_\varepsilon = \varepsilon_p/\varepsilon_m$	1
Poisson's ratio	$c_\mu = \mu_p/\mu_m$	1
Acceleration	$C_a = a_p/a_m$	1
Force	$C_F = F_P/F_m$	1000

concentrated force at the top and bottom of the model for each radial joint. In the dynamic computation, Rayleigh damping was applied. The damping coefficient of surround soil was determined by Liu [30]. The dynamic load was applied, as shown in equation (2).

To study the behavior of radial joints under long-term surface dynamic load, a model experiment was conducted. The detail of the model experiment was introduced as follows.

3.2. Physical Model Experiment Setup

3.2.1. Similitude Relation. Model experiment is an ordinary method to study the mechanical behavior and can obtain decent results. The similitude relations between the scaled model and prototype can be derived by the law of similarity for model experiment. If the dominating features of the real problem can be scaled by the model appropriately, the value of similar ratio will not significantly affect the experiment results. In the scaled model, this paper prepared, geometric dimension L, elastic modulus E, and density ρ are the 3 basic physical quantities. According to Buckingham Pi theory, other parameters such as stress, strain, force, acceleration, and time can be derived by the 3 basic physical quantities. The similitude relations can be seen in Table 3. In Table 3, C means the similitude ratio between the porotype and the model. Subscripts p and m denote the porotype and model, respectively.

3.2.2. Materials and Ratio of the Model. Plaster based material is a widely used material to simulate tunnel linings in different kinds of indoor experiments for its mechanical similarity with concrete. Fang et al. [31] conducted a physical model test the tunnel under the goaf of a thick coal seam and used a mixture of plaster and water to simulate C 25 concrete. Yang et al. [32] used a mixture of plaster, water, and kieselguhr to simulate a metro tunnel lining in a test for studying the effect of train-induced vibration for shield tunnel. Xu et al. [33] carried out a shaking table test to study the seismic response of a mountain tunnel by using plaster-based mixture to simulate the tunnel with a strength grade of C 25. Thus, the plaster-based material can be used to simulate both the cast in place and precast concrete tunnel lining under both static and dynamic loads.

According to Table 3, the scale of the porotype with respect to the physical model is 10 : 1; as a result, the length, width, and height of the model are 2.23 m, 1.4 m, and 1 m, respectively.

The mechanical properties of the model materials are significant for the model test. The test model is composed by the tunnel segment and soil. The tunnel segment with the strength grade C50 in the real project, segments in the model were fabricated by mixing water, and plaster and kieselguhr are at a ratio of 1 : 1.2 : 0.1 (by mass) materials according to the simulation rules in Table 3 by our previous study [34]. The mechanical parameters of the protype and model of the segment were shown in Table 1. The soil of the model test was fabricated by a mixture of coarse sand, quarts sand, pulverized fuel ash, and waste oil with a ratio at 1.0 : 0.8 : 0.8 : 0.3 (by mass) through a series of orthogonal tests according to the simulation rules in Table 3. The mechanical parameters of the porotype and model of the backfill soil were shown in Table 2.

The pressure applied in height direction by the bolts in the model is 0.05 MPa, according to the designed value at 0.5 MPa in the prototype and the similitude relation in Table 2. The area of each steel plate is 0.075 m^2, and the total force applied by the 5 bolts is 3750 N at each radial joint. Every prestress bolt requires to afford the force at 750 N. In the model, the prestress is applied by bolts with a diameter of 10 mm.

3.2.3. Model Fabrication and Installation. The model box was welded by steel plate with 2 mm thickness and reinforced with channel-section steel. The dimension of the model box is 3 m × 1 m × 1.4 m, as shown in Figure 4.

The underpass segments were casted in the wooden mode, with plaster slurry and kieselguhr. After 24 h, demould the segment mould. Then, the segments were dried for 72 h at 30°C.

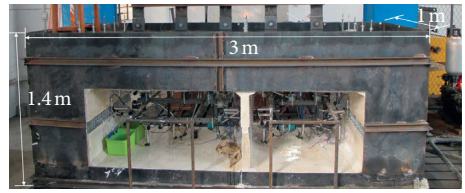

Figure 4: The dimensions of the model box.

Table 4: Prestress levels during the loading process.

Cycle numbers (million)	0~0.5	0.5~1	1~1.5	1.5~2
Prestress level (N)	375	250	125	0

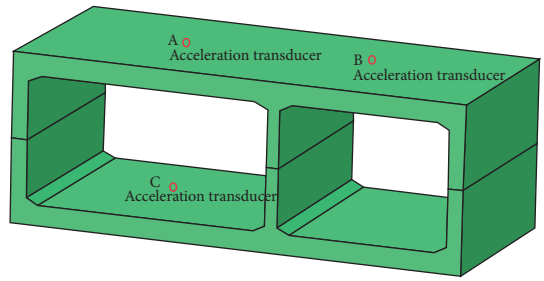

Figure 5: The layout of acceleration transducers.

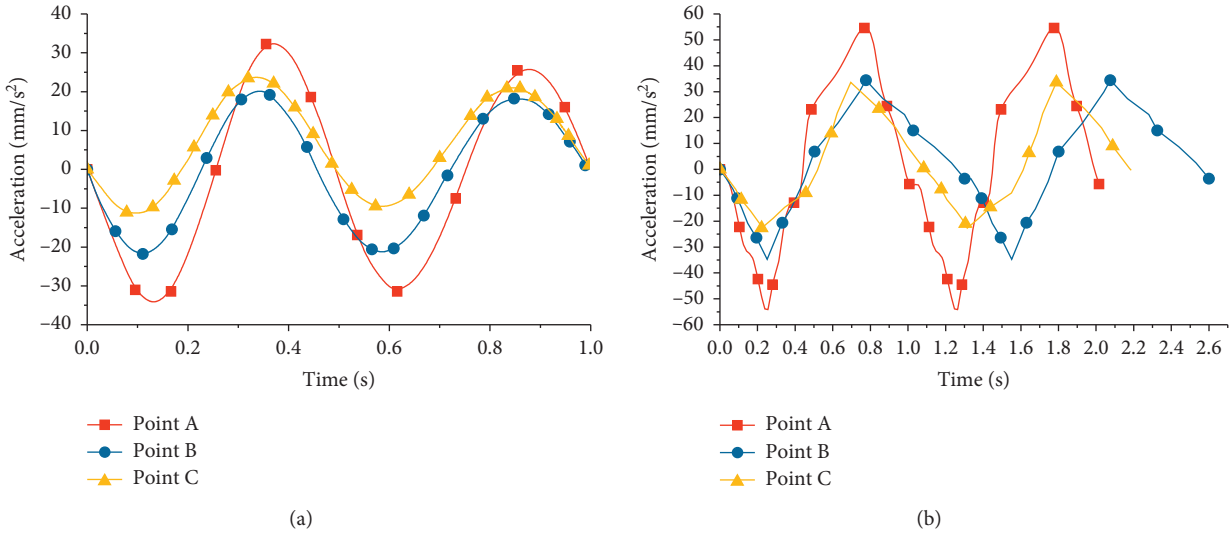

Figure 6: The response accelerations. (a) Measured results. (b) Computed results.

At the same time, the surrounding soil was configured with coarse sand, quarts sand, pulverized fuel ash, and waste oil by a blender. After the parts of the physical model were prefabricated, the installation of the parts followed the following steps. Firstly, the bottom trough of the model box was filled with plain fill and then tampered with a temper. The plain fill should be leveled to make sure the surface is flat. Secondly, the bottom segment was hoisted to specified location. Then, the top segment was assembled on the bottom segment. The prestress was applied as a designated value. Measurement sensors were installed at designated positions of the model. The side plate, front plate, and back plate were weld together. Finally, the load distributor was connected to the electronic actuator.

For a long-term study, connectors between segments will be corroded; thus, in the physical model, connectors were not considered. Connectors serve as a sealant component, not structural function.

3.2.4. Dynamic Load Selection and Input. The dynamic load was realized by a vertical actuator by a load distributor with 5 plates at the bottom which were set to simulate the five vehicles on the ground pavement.

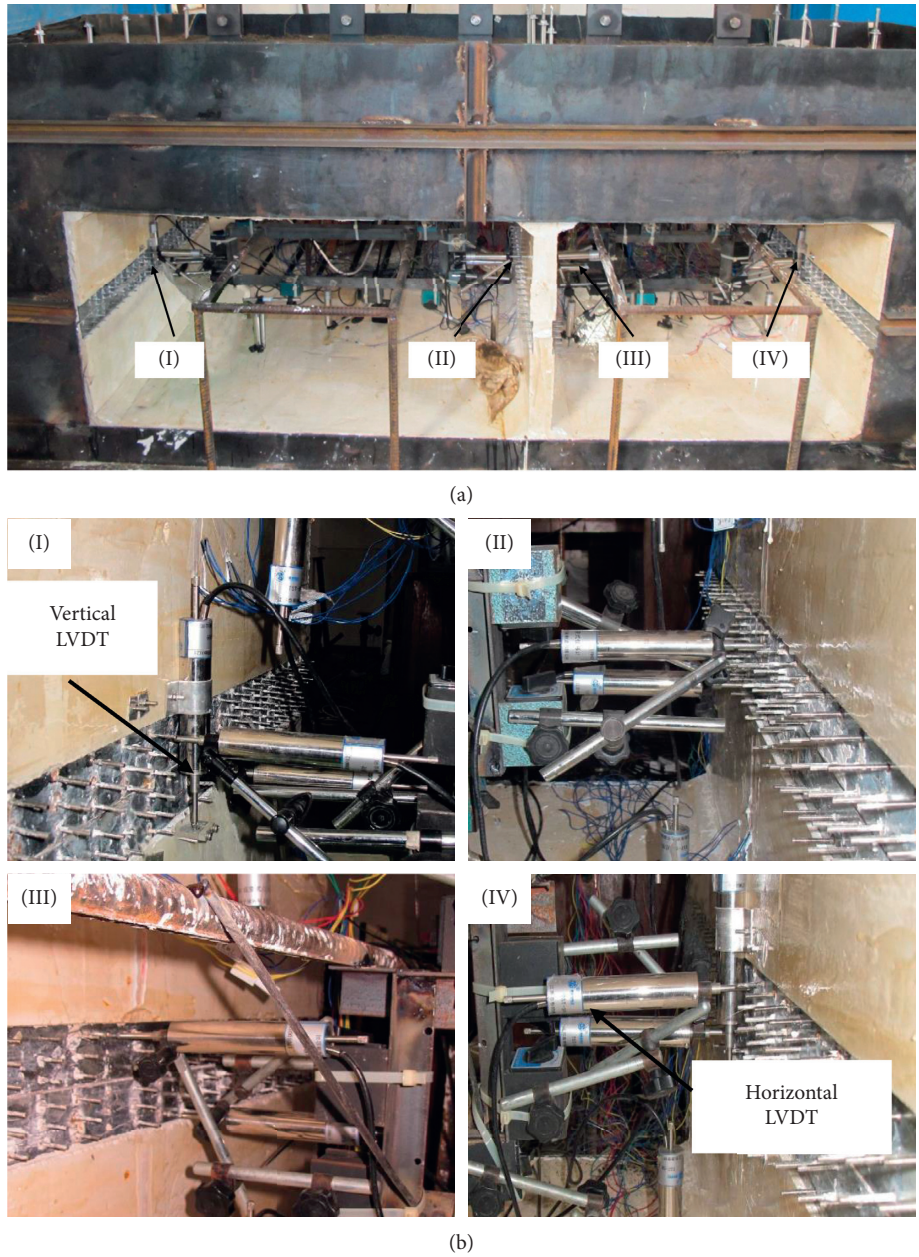

Figure 7: The layout of LVDTs around the radial joints. (a) Global view. (b) Detailed view.

Determination of the dynamic load, according to the China Code for Urban Road Design CJJ37-90, I grade the maximum of traffic load and vehicle driving speed are 700 kN and 40 km/h; thus, the loading amplitude and frequency of the model test can be calculated by the real road surcharge load and cyclic frequency and the similitude relation which were shown in Table 3.

According to equation (2) and the similitude ratio in Table 2, the amplitude and frequency of the applied load can be calculated as 700 N and 2 Hz separately. Thus, the load in physical experiment follows $700 - 700 \times \cos(2 \times \pi \times 2 \times t)$.

The cyclic number is set at 2 million times, which is an equivalent of 500,000 four-axle trucks passing through. As a permanent structure, the prestress applied the bolts between the two segments of the underpass is bound to be lost due to long-term surface traffic cyclic loads and the creep of bolts. Therefore, we considered the loss of prestress during the process of loading. The prestress was controlled, as shown in Table 4.

The model box and test field can be seen in Figures 4 and 5, respectively.

3.2.5. Monitoring System. The main purpose of this paper is to study the behavior of radial joints. These behaviors included structure dynamic response to the surface traffic load, joint opening and closing, and slipping between segments.

In order to study the dynamic response of the underpass to the ground surface vehicle loads, 3 acceleration sensors were installed at the top slab of the center of the two tubes and the center of 3 passing lane at the bottom slab,

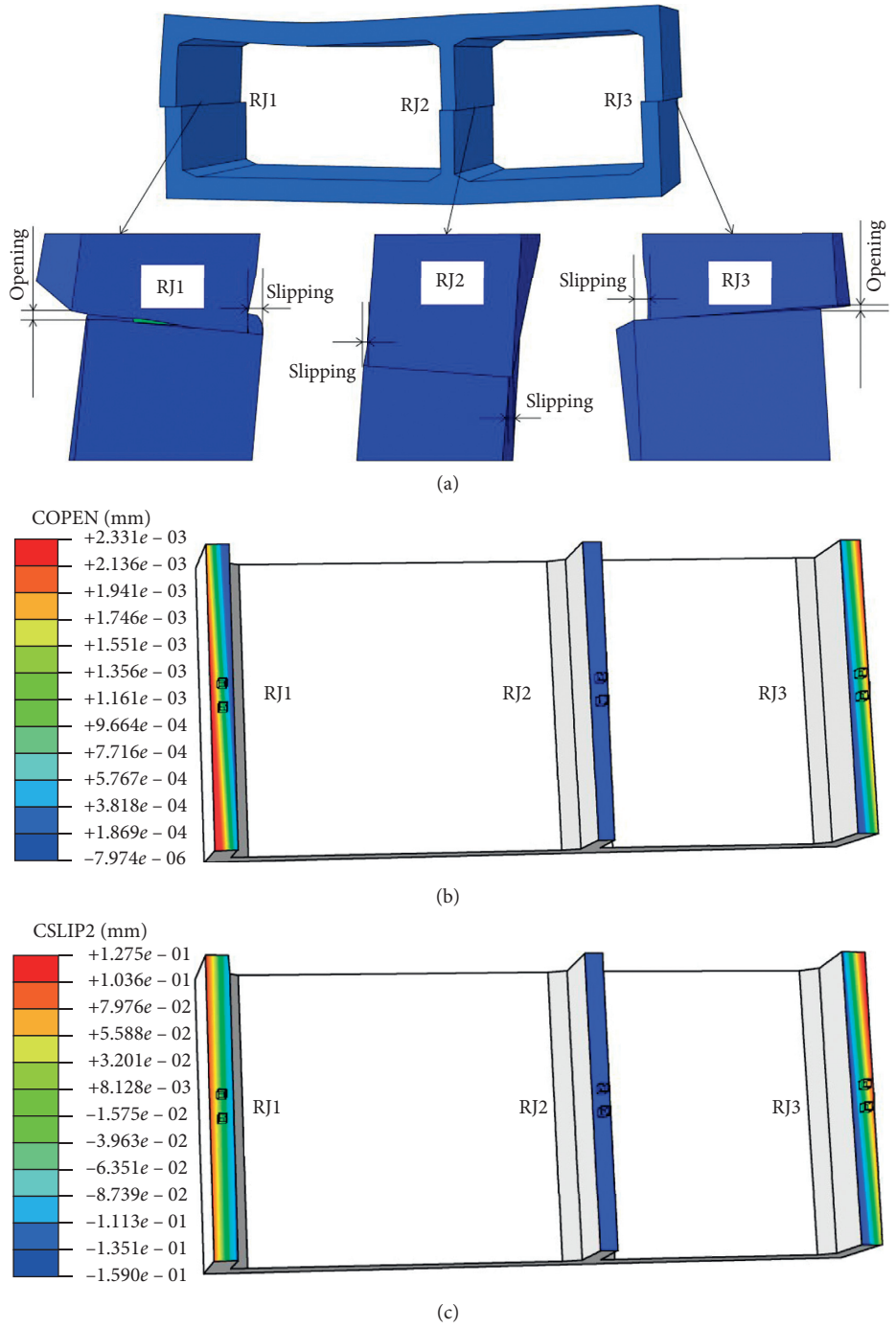

Figure 8: Radial joints displacements by numerical computation. (a) Global view. (b) Detailed joints opening. (c) Detailed joints slipping.

respectively. The layout of acceleration transducers can be seen in Figure 5.

Dynamic response of the structure was measured by three acceleration sensors located at the center of. The layout of acceleration sensors can be seen in Figure 5. The opening and closing characters of RJ's were monitored by 4 vertical Linear Variable Differential Transducers (LVDTs). For each vertical LVDT, the base was fixed on one side of the RJ and the top was contact with a steel plate flexibly. The length of the steel plate is 3 cm; thus, the lateral displacement of the RJ will not affect the measurement precise of the RJ opening and closing. The opening and closing of RJ significantly affect the sealant of the structure. Opening and closing of RJ2 was not monitored, for this joint, did not attach to the surrounding soil. Thus, the opening and closing characters were monitored in RJ 1 and RJ3. Each vertical LVDT was installed at both inside and outside of RJ1 and RJ3. The layout of vertical LVDTs was shown as Figure 6(b). The dislocation of RJ was monitored by horizontal LVDTs. Horizontal LVDTs was fixed on two steel frames. The steel

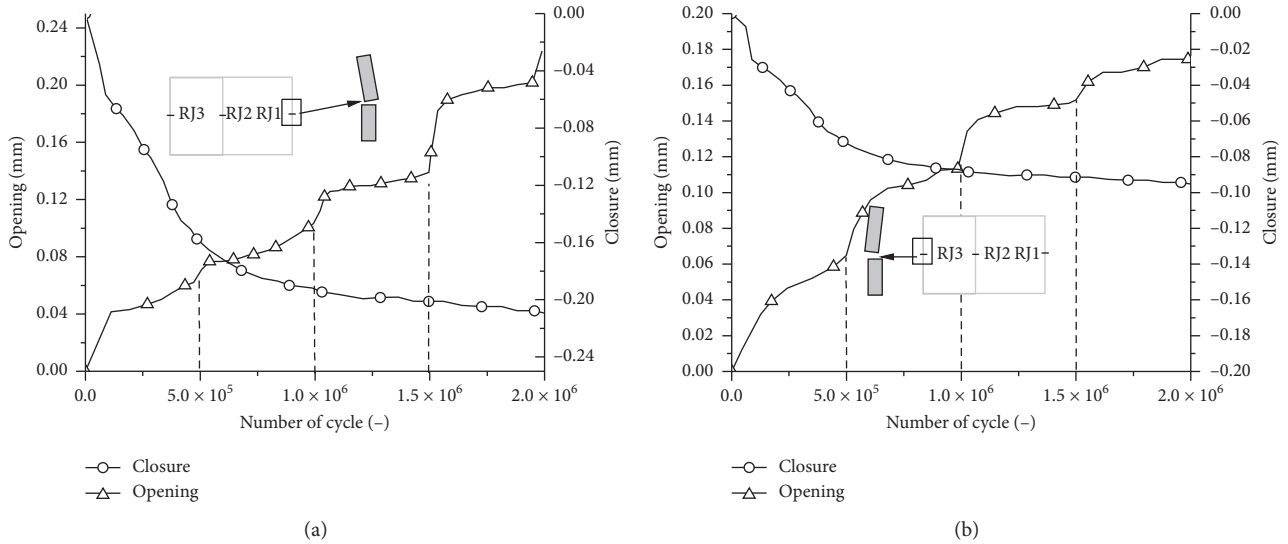

Figure 9: Joint opening at (a) RJ1 and (b) RJ3.

frames were set on the floor of the laboratory, to isolate from the model box. The layout of LVDTs can be seen in Figure 7.

4. Dynamic Response of the Plain Fill and Underpass Lining

The load on the tunnel segment may include two parts, one is the static load caused by dead load of the underpass and the surrounding soil, and the other is the dynamic load caused by ground surface vehicles. When the dynamic load reaches the pipe segment, it has not attenuated to 0, and the tunnel lining will experience a dynamic load.

In this section, the response of surface dynamic loads studied by the response acceleration and radial joints behavior. The response of acceleration and RJs behavior were monitored and measured in both the numerical model and physical model. In the following sections the computation and measured results of dynamic response and radial joints displacement were compared.

4.1. Response Acceleration of the Underpass Lining. As plotted in Figure 6, both the results of numerical simulation and model experiment (see Figure 6(b)) showed that the biggest amplitude of response acceleration was observed at point A (the center of top slab of the 3-passing lane), and the smallest one was observed at point C (the center of the bottom slab of 2-passing lane). The computed acceleration amplitudes were nearly 10 times of the measured results. The computed response periods were nearly 3 times of the measured in the model experiment. This exhibited that the simulation results were valid, according to the similitude ratio between the prototype and the model.

4.2. Radial Joints Behavior Induced by Surface Dynamic Loads. As mentioned above, the dynamic response of tunnel lining to the surface traffic is obvious. The traffic load may cause displacement in the tunnel joints. The displacement caused by dynamic loads in numerical simulation is shown in Figure 8.

In Figure 8, there are both opening and slipping occurred at RJ1 and RJ3, but there is only slipping at RJ2. At RJ 1, the top segment moves outward relative to the bottom segment, and the joint opens at the external edge. At RJ3 the joint behavior is the same as RJ1. At RJ2, the top segment moves toward to the right direction relative to the bottom segment.

The detailed joint opening can be seen in Figure 8(b). The joint opening occurred at both radial joint 1 (RJ1) and radial joint 3 (RJ3), but the opening amount of RJ1 was larger than RJ3 at the same area of the joint. However, there was no opening at RJ2.

Figure 8(c) showed the joint slipping at RJs, slipping occurred at each joint. The largest amount of slipping was at RJ1, and the smallest slipping occurred at RJ2. The negative value means the top segment moves to the right relative to the bottom segment at the joint. The positive value means the top segment moves to the left relative to the bottom segment at the joint.

The response acceleration and joint behavior induced by the dynamic load suggested that the surface traffic loads can cause dynamic effect on the underpass lining. In addition, the response acceleration of numerical simulation was consistent with the results of the model test. This convinced us that the model test can get reliable results of tunnel lining transient response induced by dynamic loads.

In Section 5, the long-term behavior of RJs under dynamic load was investigated via a model test.

5. Long-Term Behavior of Radial Joints Dynamic Loads

From Section 4 we found that the physical model experiment can reflect the real behavior of underpass RJs induced by surface vehicle loads. Hence, the model experiment was used

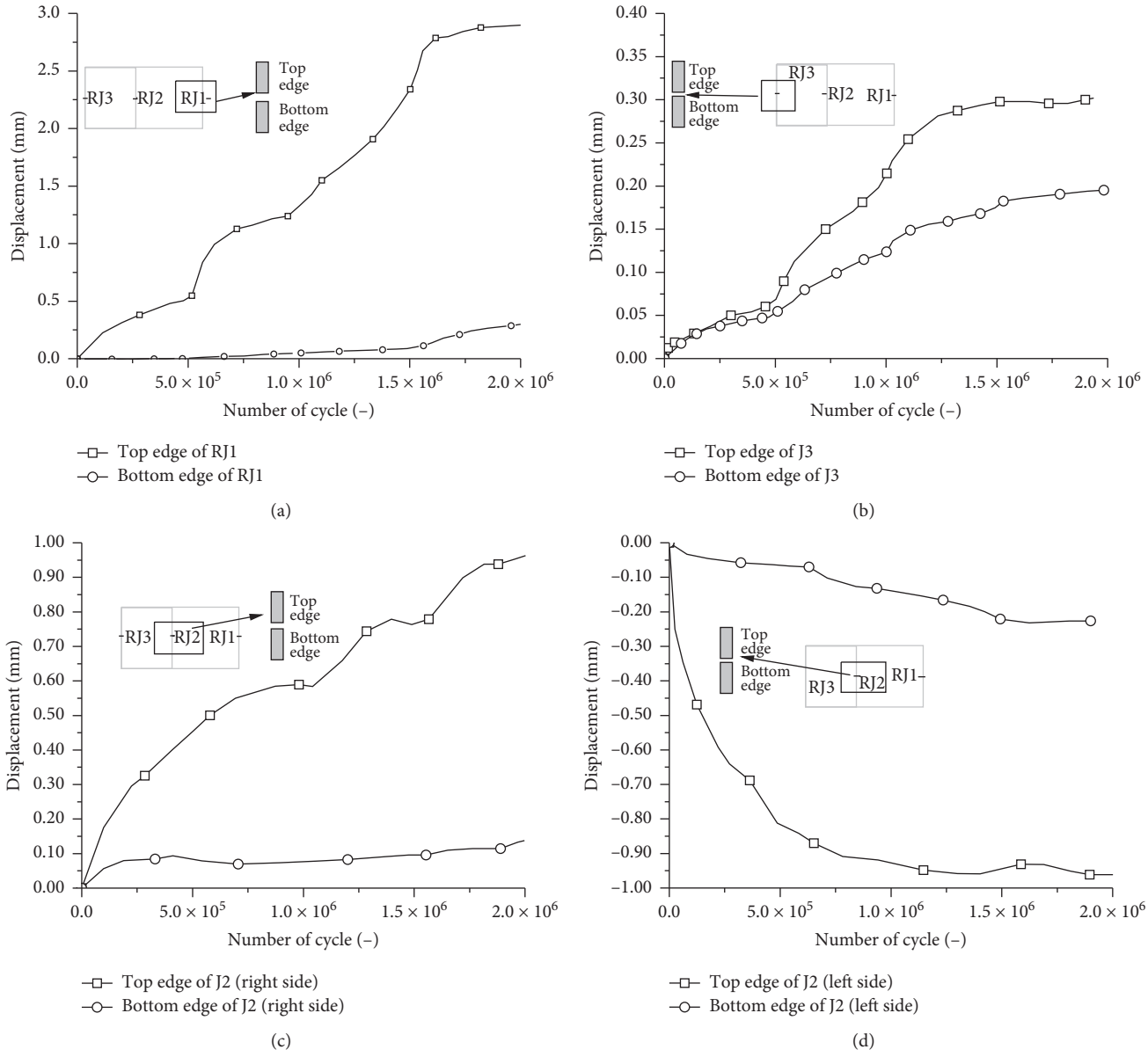

Figure 10: Joints slipping at (a) RJ1, (b) RJ3, (c) the right side of RJ2, and (d) the left side of RJ2.

to study the long-term behavior of the RJs under dynamic loads. The behavior of RLJs in our study includes the joint opening and slipping. In the following sections, characters of joint opening and slipping at RJs under long-term dynamic loads were summarized.

5.1. Joint Opening Characters at Radial Joint1 and Radial Joint 3. Figure 9(a) illustrates that the opening and closure of the radial joint at sidewall of the 3-passing lane (RJ1) of the underpass. The opening at RJ1 increases at a higher speed, this mainly attributed to the readjustment of contact relationship of the joint surfaces. The opening at RJ1 increased slowly from 0.12×10^6 to 1×10^6, while the opening has a sharp rise shortly after 1.0×10^6 and 1.5×10^6; this may be caused by the release of prestress at the joint. The prestress is released firstly at 0.5×10^6, but the prestress is still at a high level after 0.5×10^6. The most drastic rise occurs at 1.5×10^6, after which the prestress is released to 0. This means that for RJ1 the prestress should not be less than that at 1.0×10^6–1.5×10^6 interval. The slop of the opening curve becomes the steepest at the end of the test. The closure curve of the RJ3 shows a decline tendency during the whole test process, the accumulative closure of first 1×10^6 accounts for more than 3/4 of the total closure. This means the closure rate decreased with the increase of accumulative closure of the joint. There are two possible reasons for this tendency, one is the unevenness of the joint contact surface decreases with the increase in the amount of closure and the number of cycles; another maybe the whole structure becomes more stable with the increase of loading cycles. Comparison of Figures 9(a) and 9(b) suggests that the characters of

accumulative opening and closure at RJ3 are nearly the same as RJ1, whereas the total amount of opening and closure at RJ1 is larger than that at RJ3 which caused by the shorter span length at RJ3 than that at RJ1. Therefore, the accumulative opening and closure show an asymmetric effect.

5.2. Joint Slipping Characters. Figure 10 plots that the horizontal deformation of the segments at RJ1, RJ3, and 2 sides of RJ2. The results show that at each joint the horizontal deformation at the top segment is larger than that of bottom segment. This means that the horizontal deformation at the top segment is the source of the horizontal deformation at the joint. The deformation increases at a high level and then is decreased with the increase of accumulative deformation; this may be caused by the gap between of the outsider of the shear keys and the insider of the holes to install the shears keys. When the amount of deformation of the upper segment reaches a certain value, the contact surfaces of shear keys and the hole fit together, and then the shear keys start to work, the deformation decreases. Another possible reason is that the stiffness of soil increases with the increase of the deformation at the joints which in turn provides stronger restrain for the joints.

6. Conclusions

In order to study the radial joints behavior of a shallow buried large cross-section underpass under long-term dynamic loads from the ground surface. Based on a real underpass crossing beneath the south section of the first ring road in Chengdu, a numerical model was constructed and a 1/10 scaled model experiment was conducted. From the analysis of the results both from numerical computation and experiment, following conclusions can be drawn:

(1) According to the response accelerations of both the numerical and model experiment, the results from numerical simulation are in good accordance with that of model experiment, which convinces us that the numerical simulation is valid.

(2) The characters of radial joint displacement were investigated by numerical and model experiment. Both the results exhibited the same characters; the displacement consisted of joint opening and sipping; opening and slipping occurred at RJ1 (sidewall of the 3 passing lane) and RJ3 (sidewall of the 2 passing lane), but there was only slipping at RJ2 (middle wall of the structure).

(3) Although the characters of the behavior of RJ1 and RJ3 are similar, the values of opening and slipping are different, and both the values of long-term opening and slipping at RJ1 are greater than that at RJ3 which mainly due to the wider span of RJ1.

(4) The model experiment demonstrated that the joint opening is closely correlated with the prestress level, and the larger the prestress, the smaller the opening. The relationship between the joint slipping and prestress level is not that significant as the relationship between the joint opening and prestress level.

Data Availability

The data used to support the findings of this study are available from the corresponding author upon request.

Conflicts of Interest

The authors declare that there are no conflicts of interest regarding the publication of this paper.

Acknowledgments

We would like to thank National Natural Science Foundation of China (Grant nos. 51478395, 51678490, and 5197080874) for the financial support. The anonymous referees would likely to be acknowledged by the authors for their evaluation of the paper.

References

[1] M. H. Baziar, M. R. Moghadam, D.-S. Kim, and Y. W. Choo, "Effect of underground tunnel on the ground surface acceleration," *Tunnelling and Underground Space Technology*, vol. 44, pp. 10–22, 2014.

[2] U. Cilingir and S. P. G. Madabhushi, "A model study on the effects of input motion on the seismic behaviour of tunnels," *Soil Dynamics and Earthquake Engineering*, vol. 31, no. 3, pp. 452–462, 2011.

[3] W. Yang, L. Li, Y. Shang et al., "An experimental study of the dynamic response of shield tunnels under long-term train loads," *Tunnelling and Underground Space Technology*, vol. 79, pp. 67–75, 2018.

[4] J. Lai, K. Wang, J. Qiu, F. Niu, J. Wang, and J. Chen, "Vibration response characteristics of the cross tunnel structure," *Shock and Vibration*, vol. 2016, pp. 1–16, 2016.

[5] L. J. Tao, P. Ding, C. Shi, X. W. Wu, S. Wu, and S. C. Li, "Shaking table test on seismic response characteristics of prefabricated subway station structure," *Tunnelling and Underground Space Technology*, vol. 91, Article ID 102994, pp. 1–25, 2019.

[6] P. Ding, L. Tao, X. Yang, J. Zhao, and C. Shi, "Three-dimensional dynamic response analysis of a single-ring structure in a prefabricated subway station," *Sustainable Cities and Society*, vol. 45, pp. 271–286, 2019.

[7] Y. B. Lai, M. S. Wang, X. H. You, and Z. Y. He, "Overview and outlook for protection and prefabrication techniques of tunnel and underground projects," *Building Technique Development*, vol. 42, no. 1, pp. 24–28, 2015.

[8] N. S. Rasmussen, "Concrete immersed tunnels - forty years of experience," *Tunnelling and Underground Space Technology*, vol. 12, no. 1, pp. 33–46, 1997.

[9] D. C. Wang, G. F. Wang, N. Qiao, and C. S. Dai, "The application and prospect analysis of prefabricated construction in underground engineering," *China Sciencepaper*, vol. 13, no. 1, pp. 115–119, 2018.

[10] H. M. Liu, *Study on Mechanical Properties of Assembled Lining in Open-Cut Section of Underground Railway*, Master's thesis, Southwest Jiaotong University, Chengdu, China, 2003.

[11] M. N. Wang, Z. Y. Li, and B. S. Guan, "Study on prefabricated concrete lining technology for open trench subway tunnels," *Journal of China Railway Society*, vol. 26, no. 3, pp. 88–92, 2004.

[12] P. Yurkevich, "Developments in segmental concrete linings for subway tunnels in belarus," *Tunnelling and Underground Space Technology*, vol. 10, no. 3, pp. 353–365, 1995.
[13] B. G. Casteren, *Feasibility of Prefabricated Concrete Elements for Underpasses*, M.S.C.E. thesis, Delft University of Technology, Rotterdam, Netherlands, 2015.
[14] A. Caratelli, A. Meda, Z. Rinaldi, S. Giuliani-Leonardi, and F. Renault, "On the behavior of radial joints in segmental tunnel linings," *Tunnelling and Underground Space Technology*, vol. 71, pp. 180–192, 2018.
[15] R. L. Wang and D. M. Zhang, "Mechanism of transverse deformation and assessment index for shield tunnels in soft clay under surface surcharge," *Chinese Journal of Geotechnical Engineering*, vol. 36, pp. 1092–1101, 2013.
[16] R. L. Wang, "Longitudinal deformation analysis for Shanghai subway tunnel constructed by shield method," *Underground Engineering and Tunnels*, vol. 4, pp. 1–7, 2009.
[17] F. I. Shalabi, E. J. Cording, and S. L. Paul, "Concrete segment tunnel lining sealant performance under earthquake loading," *Tunnelling and Underground Space Technology*, vol. 31, pp. 51–60, 2012.
[18] X. Li, Z. Yan, Z. Wang, and H. Zhu, "A progressive model to simulate the full mechanical behavior of concrete segmental lining longitudinal joints," *Engineering Structures*, vol. 93, pp. 97–113, 2015.
[19] X. Li, Z. Yan, Z. Wang, and H. Zhu, "Experimental and analytical study on longitudinal joint opening of concrete segmental lining," *Tunnelling and Underground Space Technology*, vol. 46, pp. 52–63, 2015.
[20] J. Sun and X. Y. Hou, "Design theory and practice of circular tunnels in Shanghai area," *China Civil Engineering Journal*, vol. 17, no. 8, pp. 35–47, 1984.
[21] H. Huang, H. Shao, D. Zhang, and F. Wang, "Deformational responses of operated shield tunnel to extreme surcharge: a case study," *Structure and Infrastructure Engineering*, vol. 13, no. 3, pp. 345–360, 2017.
[22] H. Yi, T. Qi, W. Qian et al., "Influence of long-term dynamic load induced by high-speed trains on the accumulative deformation of shallow buried tunnel linings," *Tunnelling and Underground Space Technology*, vol. 84, pp. 166–176, 2019.
[23] Y. Jin, W. Ding, Z. Yan, K. Soga, and Z. Li, "Experimental investigation of the nonlinear behavior of segmental joints in a water-conveyance tunnel," *Tunnelling and Underground Space Technology*, vol. 68, pp. 153–166, 2017.
[24] X. Liu, Y. Bai, Y. Yuan, and H. A. Mang, "Experimental investigation of the ultimate bearing capacity of continuously jointed segmental tunnel linings," *Structure and Infrastructure Engineering*, vol. 12, no. 10, pp. 1364–1379, 2016.
[25] X. J. Deng, "Study on dynamics of vehicle-ground pavement structure system," *Journal of Southeast University (Natural Science Edition)*, vol. 32, pp. 474–479, 2002.
[26] Y. Cai, Y. Chen, Z. Cao, H. Sun, and L. Guo, "Dynamic responses of a saturated poroelastic half-space generated by a moving truck on the uneven pavement," *Soil Dynamics and Earthquake Engineering*, vol. 69, pp. 172–181, 2015.
[27] L. Sun and X. Deng, "Predicting vertical dynamic loads caused by vehicle-pavement interaction," *Journal of Transportation Engineering*, vol. 124, no. 5, pp. 470–478, 1998.
[28] H. Chen, "Dynamic finite element analysis of highway subgrade under traffic load," Master's thesis, Southwest Jiaotong University, Chengdu, China, 2003.
[29] ABAQUS Inc., "ABAQUS user's manual-version 2016," 2010.
[30] Y. X. Liu, "Study on fatigue failure form and life prediction of shield segment under high-speed train dynamic load," Master's thesis, Southwest Jiaotong University, Chengdu, China, 2017.
[31] Y. Fang, Z. Yao, G. Walton, and Y. Fu, "Liner behavior of a tunnel constructed below a caved zone," *KSCE Journal of Civil Engineering*, vol. 22, no. 10, pp. 4163–4172, 2018.
[32] W. B. Yang, Z. Q. Chen, Z. Xu, Q. X. Yan, C. He, and W. Kai, "Dynamic response of shield tunnels and surrounding soil induced by train vibration," *Rock and Soil Mechanics*, vol. 39, no. 2, pp. 537–545, 2018.
[33] H. Xu, T. Li, L. Xia, J. X. Zhao, and D. Wang, "Shaking table tests on seismic measures of a model mountain tunnel," *Tunnelling and Underground Space Technology*, vol. 60, pp. 197–209, 2016.
[34] W. P. Qian, T. Y. Qi, H. Y. Yi et al., "Evaluation of structural fatigue properties of metro tunnel by model test under dynamic load of high-speed railway," *Tunnelling and Underground Space Technology*, vol. 93, Article ID 103099, pp. 1–16, 2019.